Available online at www.sciencedirect.com
ScienceDirect
Intermetallics 15 (2007) 442–450
Intermetallics
www.elsevier.com/locate/intermet

Short Communication

A new class of tailor-made $Fe_{0.92}Mn_{0.08}Si_2$ lithium battery anodes: Effect of composite and carbon coated $Fe_{0.92}Mn_{0.08}Si_2$ anodes

N. Jayaprakash [a], N. Kalaiselvi [a,*], C.H. Doh [b]

[a] *Central Electrochemical Research Institute, Karaikudi 630 006, India*
[b] *Korea Electrotechnology Research Institute, Changwon 641 600, South Korea*

Received 28 March 2006; received in revised form 5 July 2006; accepted 23 August 2006
Available online 27 October 2006

Abstract

As an approach to surpass the unavoidable capacity fading of native silicon anodes upon cycling, newer anodes such as $FeSi_2$ (alloy anode), $Fe_{0.92}Mn_{0.08}Si_2$ (doped alloy anode), $FeSi_2$/graphite and $Fe_{0.92}Mn_{0.08}Si_2$/graphite composite anodes were prepared via mechanical ball milling process. Subsequently, coating of disordered carbon on the parent $FeSi_2$ and $Fe_{0.92}Mn_{0.08}Si_2$ matrix was carried out through the pyrolysis of PVC. The introduction of co-milling component (8% manganese) as dopant into the parent $FeSi_2$ structure was found to enhance only the specific capacity values of native $FeSi_2$ anodes during the initial cycles, whereas the deployment of composite alloy anodes ($FeSi_2$/graphite and $Fe_{0.92}Mn_{0.08}Si_2$/graphite) and the carbon coated $FeSi_2$ and $Fe_{0.92}Mn_{0.08}Si_2$ anodes has exhibited good cyclic reversibility (<10%) and excellent coulombic efficiency (>95%) values upon extended cycling. From the set of alloy anodes chosen for the present study, $Fe_{0.92}Mn_{0.08}Si_2$/graphite composite seems to have promising anode capability with an initial discharge capacity of 547 mAh/g followed by minimal capacity fade. It is believed that graphite plays an important role of buffering the volume expansion of alloy anodes and the carbon coating enhances the interface strength between electrode active material and current collector so as to realize improved electrochemical properties of alloy anodes upon extended cycling.

Keywords: A. Silicides, various; A. Composites; B. Surface properties; C. Mechanical alloying and milling; F. Scanning tunneling electron microscopy

1. Introduction

It is well known that the demand for lithium-ion batteries with volume based energy density and as a power supply for the portable electronic devices is increasing at a faster rate. Catering to this demand could be possible only by replacing the currently used carbon with some other alternative anode material for known reasons [1]. In this regard, fourth group elements, particularly Sn and Si are expected to react with far more lithium and there by gather considerable attention from recent researchers [1,2]. Basically, lithium alloy which has high volumetric and gravimetric capacities due to their high lithium packing density and safe thermodynamic potential compared to the carbonaceous material like graphite has been studied extensively [3–5]. Silicon that can react with lithium to form an alloy with a high Li/Si ratio at elevated temperatures is reported to yield a variety of compounds such as $Li_{12}Si_7$, $Li1_3Si_4$, Li_7Si_3, and $Li_{22}Si_5$ [6,7]. Among them, the theoretical capacity of $Li_{22}Si_5$ is around 4200 mAh/g, which is the highest capacity ever reported in the literature for any of the Li alloys known till date [8]. On the other hand, the volume expansion of silicon is greater than any other material, which results in the mechanical pulverization of the active material and leads to a rapid capacity fading in the succeeding cycles. Therefore, several attempts are being made to improve the cycleability of silicon anodes [9–15], with a view to

* Corresponding author. Tel.: +91 4565 227550–559; fax: +91 4565 227779.
E-mail address: kalakanth2@yahoo.com (N. Kalaiselvi).

0966-9795/$ - see front matter © 2006 Published by Elsevier Ltd.
doi:10.1016/j.intermet.2006.08.014

circumvent the hampering issue of exorbitant volume expansion. Yoshio et al. have attempted to improve the life cycle of silicon by coating the surface of fine powders of Si with CVD deposited carbon [16], but encountered with yet another problem related to the need to keep an exact charging potential. However, Lee and co-workers succeeded in improving the cycleability, which appeared to be insufficient for practical use [17]. The use of nano-sized Si particle to overcome the hampering issues was also proved to be less effective as shown by Li et al. [18]. Therefore, it is deduced that the use of tailor-made silicon based alloy with a larger inactive atom matrix (M_xSi_y) and smaller active center (Si) could suppress the volume expansion effectively [19], so as to achieve better cycleability and capacity retention behavior.

With this background, $FeSi_2$ alloy has been tried as the possible anode material for lithium-ion battery, in which Si emerges out as the active center and $FeSi_2$ as inactive host matrix materials. The study highlights the synthesis, characterization and explores the possible extent to which the electrochemical performance characteristics of $FeSi_2$ could be improved. Herein, two different approaches viz., preparing a composite anode of $FeSi_2$ with graphite and the incorporation of Mn as a dopant to partially replace Fe to form $Fe_{0.92}Mn_{0.08}Si_2$ were adopted with a view to modify the electrochemical behavior of native $FeSi_2$. Based on the encouraging results obtained from the electrochemical behavior of $FeSi_2$/graphite composite anode, it was planned further to synthesize and to investigate the electrochemical behavior of $Fe_{0.92}Mn_{0.08}Si_2$/graphite composite anode also. As a result, effect of composite anodes and the synergetic effects of dopant (Mn) and composite anode were studied individually from $FeSi_2$/graphite composite anode and from the $Fe_{0.92}Mn_{0.08}Si_2$/graphite composite anode, respectively. Further, having intrigued by the earlier reports of the same authors concerned with the possibility of enhancing the electrochemical behavior of Cu_6Sn_5 alloy anodes through pyrolysed carbon coating [20], it was felt that the effect of carbon coating on the selected set of parents viz., $FeSi_2$ and $Fe_{0.92}Mn_{0.08}Si_2$ would be more interesting. As a result, carbon coated $FeSi_2$ and $Fe_{0.92}Mn_{0.08}Si_2$ electrode materials were also synthesized, investigated for electrochemical properties and compared with those of the composite and doped alloy anodes of $FeSi_2$.

All the synthesized compounds were subjected to both physical (XRD, SEM) and electrochemical characterization (charge–discharge) studies systematically to understand the effects of doping ($Fe_{0.92}Mn_{0.08}Si_2$), composite anodes ($FeSi_2$/graphite and the $Fe_{0.92}Mn_{0.08}Si_2$/graphite) and the effect of carbon coating (carbon coated $FeSi_2$ and $Fe_{0.92}Mn_{0.08}Si_2$ compounds) individually against lithium metal.

2. Experimental

2.1. Synthesis procedure

Fig. 1 shows the schematic representation of the entire process involved in the synthesis of variety of anode active materials chosen for the study. An easy-to-adopt mechanical alloying method has been deployed to synthesize $FeSi_2$, $Fe_{0.92}Mn_{0.08}Si_2$, $FeSi_2$/graphite and $Fe_{0.92}Mn_{0.08}Si_2$/graphite composite anodes individually. Further, carbon coating has been carried out through the pyrolysis of PVC, a polymer with no oxygen content in order to avoid the risk of oxidation

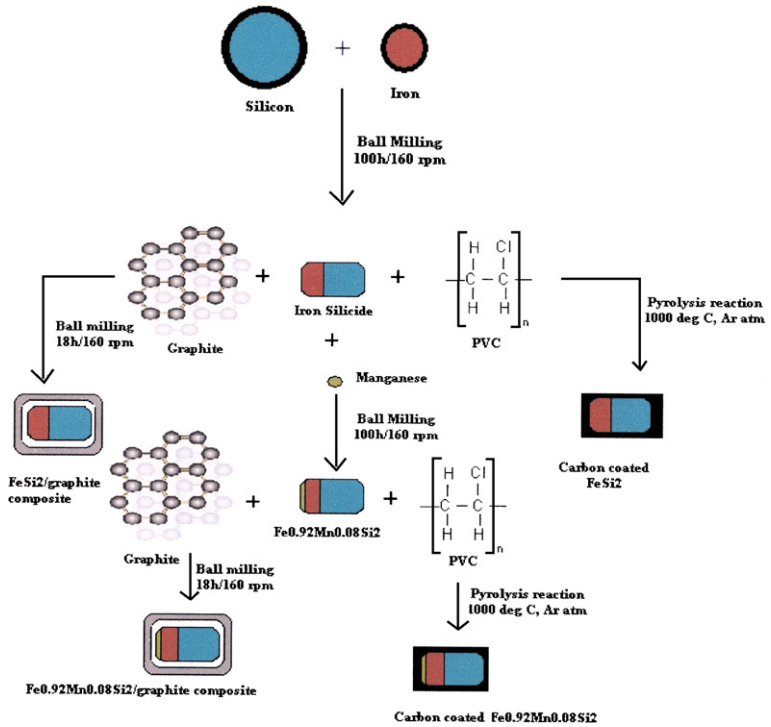

Fig. 1. Schematic representation of the process involved in the synthesis of the active material.

upon decomposition of the polymer, which is the highlight of this study. Even though it is reported that carbon coating through propylene carbonate based electrolyte could reduce the irreversible capacity of anodes [21], disordered carbon coating through the pyrolysis of PVC has been chosen for the study, based on the fact that porous PVC polymer would absorb the alloy/graphite composite precursor effectively [22].

Analytical grade powders of Fe, Mn and Si (99.9% pure, Sigma Aldrich, South Korea) were taken in the stoichiometric ratio, 0.92:0.08:2, in a container meant for planetary ball mill, with zirconium balls of two different sizes (in the ratio of 2:4) to ensure complete milling and to yield finer particle size. The container was air sealed with paraffin films to prevent the entry of atmospheric air that might lead to the oxidation of alloy material. Subsequently, argon gas was passed into the container at a constant rate for 30 min to flush out the residual air present inside the container. Then the argon filled container was fixed into the planetary ball mill and allowed to run for 100 h at 160 rpm. The as milled fine alloy powder was taken out and sieved with grinding for equal particle size distribution.

2.2. Graphite coating

The ball milled $FeSi_2$ and $Fe_{0.92}Mn_{0.08}Si_2$ alloy samples were mixed with graphite (Dag-68, Sodiff, 1:1 ratio) and were subjected to ball milling for 18 h at 160 rpm in the planetary ball mill in the same manner as mentioned above. The $FeSi_2$/graphite and $Fe_{0.92}Mn_{0.08}Si_2$/graphite composite materials thus obtained were taken out, sieved and subjected to characterization studies.

2.3. Carbon coating

Finally, carbon coating of the alloy was carried out via mixing the $FeSi_2$ or $Fe_{0.92}Mn_{0.08}Si_2$ alloy with 70 wt% PVC in a mortar and heating the mixture at 800–1000 °C under argon flow for 1 h in an alumina heating boat. The heating rate was 10 °C per minute and the sample was taken out and ground further to obtain ultra fine powders of carbon coated $FeSi_2$ or $Fe_{0.92}Mn_{0.08}Si_2$ alloy individually.

2.4. Physical and electrochemical characterization

Phase characterization was done by powder X-ray diffraction technique on a Philips 1830 X-ray diffractometer using Ni filtered Cu K_α radiation ($\lambda = 1.5406$) in the 2θ range of 10°–120° at a scan rate of 0.04°/s. Surface morphology of the particles was examined through SEM images obtained from Jeol S-300 H scanning electron microscope and actual size of the particles was measured using Malvern easy particle size analyzer. Charge–discharge studies were carried out using Maccor charge–discharge cycler.

2.5. Electrode preparation and coin cell fabrication

Electrochemical charge–discharge evaluation was done on 2016 coin cells fabricated using the synthesized anodes and Li metal. The electrodes were made by dispersing 90 wt% of active material and 10 wt% of poly(vinylidene fluoride) (PVDF) binder in *N*-methyl-2-pyrrolidone (NMP) solvent. The resulting slurry was spread on a copper foil, dried for 12 h to remove the excess of NMP and then hot roll pressed into sheets. 2016 coin cells were fabricated with the electrodes punched out from the sheet and lithium was used as the counter electrode. EC/DMC/EMC/PC (4/3/3/1 by vol.) dissolved in 1.0 M $LiPF_6$ electrolyte (Cheil Industries Ltd, South Korea) and Asaki polypropylene separator were used.

3. Results and discussion

3.1. Phase formation results – XRD analysis

Presence of broad and well defined peaks at $2\theta = 29°$ and 45° is the striking evidence, respectively, for the formation of size controlled $FeSi_2$ and $Fe_{0.92}Mn_{0.08}Si_2$ alloy particles (Figs. 2a and 3a). Similarly, $FeSi_2$/graphite and $Fe_{0.92}Mn_{0.08}Si_2$ alloy/graphite composite powder obtained after 18 h of ball milling also exhibited characteristic and broader peaks, as evident from Figs. 2b and 3b. This may be attributed to the prolonged and high speed pulverization of mechanical alloying process that has played a vital role against particle agglomeration and to yield ultra fine powders. In other words, all the ball milled products, viz., $FeSi_2$, $FeSi_2$/graphite, $Fe_{0.92}Mn_{0.08}Si_2$ and $Fe_{0.92}Mn_{0.08}Si_2$/graphite powders are expected to possess smaller size of the particles well within the desired micron level (<10 μm). On the other hand, carbonization of PVC that occurs above 500 °C is found to slightly increase the crystalline size, despite the monotonic decrease of h/c atomic ratio especially at 1000 °C [22]. Therefore, the carbon that has been coated over the alloy is expected to have disordered or amorphous nature, as reported by Lee et al. [21].

It is noteworthy that no significant difference has been observed with the XRD pattern of $FeSi_2$ (Fig. 2a) and Mn doped $FeSi_2$ (Fig. 3a) and the presence of Mn was also not obvious from the entire set of $Fe_{0.92}Mn_{0.08}Si_2$ derivatives (Fig. 3a–c), which are due to the lower volumetric fraction and the finer dispersion of Mn throughout the matrix of $FeSi_2$ [23]. Similarly, based on the restricted broadening of Bragg peaks observed for the native alloy ($FeSi_2$), doped alloy ($Fe_{0.92}Mn_{0.08}Si_2$) and the alloy/graphite composite powders ($FeSi_2$/graphite and $Fe_{0.92}Mn_{0.08}Si_2$/graphite) (Figs. 2a, 3a, 2b and 3b, respectively), it is understood that the process of ball milling is found to be effective in controlling the size of the individual particles to some extent, as expected. On the other hand, the process of pyrolysis carried out at high calcination temperature that does not seem to have any significant control against the growth of particles has exhibited sharp and narrow peaks, as evident from the Bragg patterns recorded for carbon coated $FeSi_2$ (Fig. 2c) and $Fe_{0.92}Mn_{0.08}Si_2$ alloy anode powder (Fig. 3c). This is an indication for the possible presence of size grown particles due to the high temperature (1000 °C) treatment, as mentioned already.

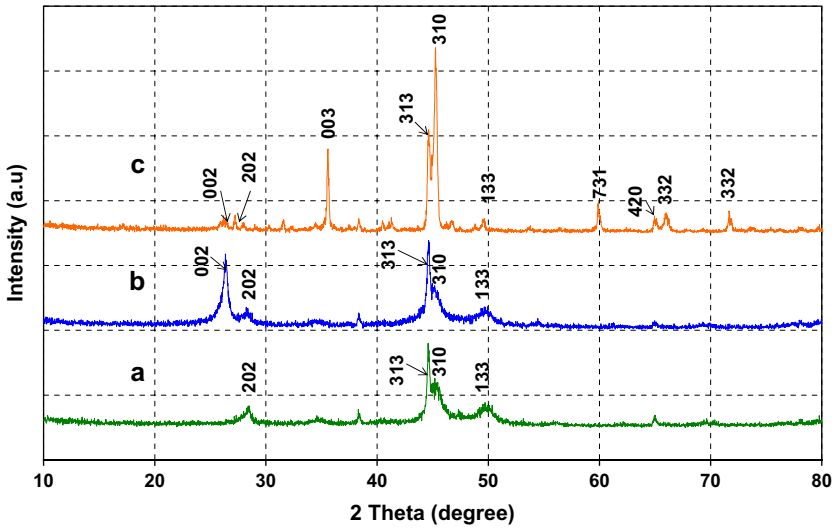

Fig. 2. XRD pattern of $FeSi_2$ alloy and its composite material (a) $FeSi_2$ alloy, (b) $FeSi_2$/graphite composite and (c) carbon coated $FeSi_2$.

3.2. Morphological results – SEM study

The scanning electron microscopic (SEM) images of the as ball milled $FeSi_2$ alloy and its derivatives such as $FeSi_2$/graphite, carbon coated $FeSi_2$ are depicted in Fig. 4a–c. Similarly, the SEM images of the doped alloy ($Fe_{0.92}Mn_{0.08}Si_2$) and its corresponding derivatives such as $Fe_{0.92}Mn_{0.08}Si_2$ alloy/graphite and carbon coated $Fe_{0.92}Mn_{0.08}Si_2$ are shown in Fig. 5a–c. Presence of spherical grains with definite grain boundaries and the uniform distribution of graphite/coated carbon over the surface of $FeSi_2$ and $Fe_{0.92}Mn_{0.08}Si_2$ alloys are obvious from the captured images (Figs. 4 and 5). Particularly, the perfect wrapping or coating of the amorphous carbon over the surface of the $FeSi_2$ and $Fe_{0.92}Mn_{0.08}Si_2$ alloy is clearly seen from Figs. 4c and 5c. Also, the particle size of the alloys, alloy composites and carbon coated alloys was found to present well within the expected <10 μm level, which is the significant feature of all the compounds synthesized through the present study.

The presence of uniformly distributed, size reduced particles of the alloys and their derivative composites as inferred from SEM has further been confirmed through particle size analysis. With a view to understand the exact size region in which the individual particles of the alloys get distributed, the particle size distribution plot of the as ball milled $FeSi_2$ alloy and its derivatives such as FeSi2/graphite and carbon coated $FeSi_2$ is furnished in Fig. 6a–c. Similarly, particle size distribution results of the doped alloy ($Fe_{0.92}Mn_{0.08}Si_2$) and its corresponding derivatives such as $Fe_{0.92}Mn_{0.08}Si_2$ alloy/graphite and carbon coated $Fe_{0.92}Mn_{0.08}Si_2$ are shown in Fig. 7a–c.

It is quite interesting to note that all the particles are found to possess the average particle size distribution of 4–9 μm, which is a favorable property to exhibit better electrochemical performance. Therefore, as mentioned in PXRD results, the process of ball milling has significant effect over the size control of mechanically alloyed $FeSi_2$, $Fe_{0.92}Mn_{0.08}Si_2$ alloy and

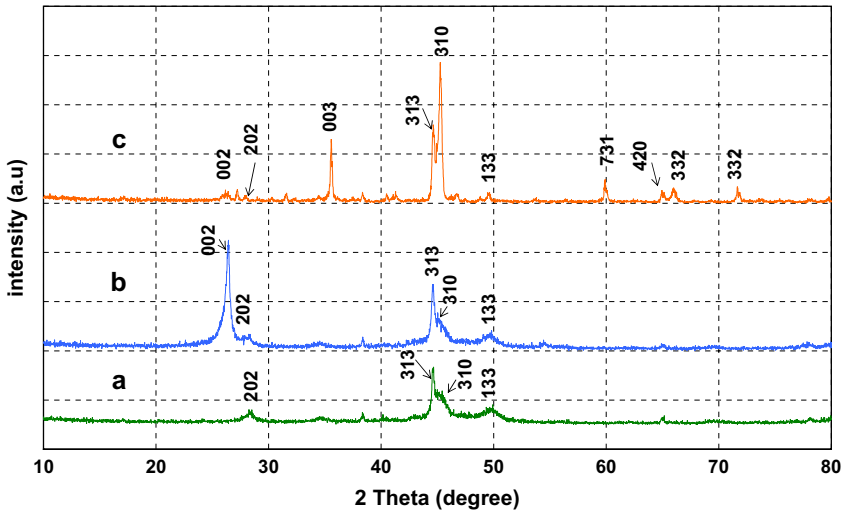

Fig. 3. XRD pattern of $Fe_{0.92}Mn_{0.08}Si_2$ alloy and its composite material (a) $Fe_{0.92}Mn_{0.08}Si_2$ alloy, (b) $Fe_{0.92}Mn_{0.08}Si_2$/graphite composite and (c) carbon coated $Fe_{0.92}Mn_{0.08}Si_2$.

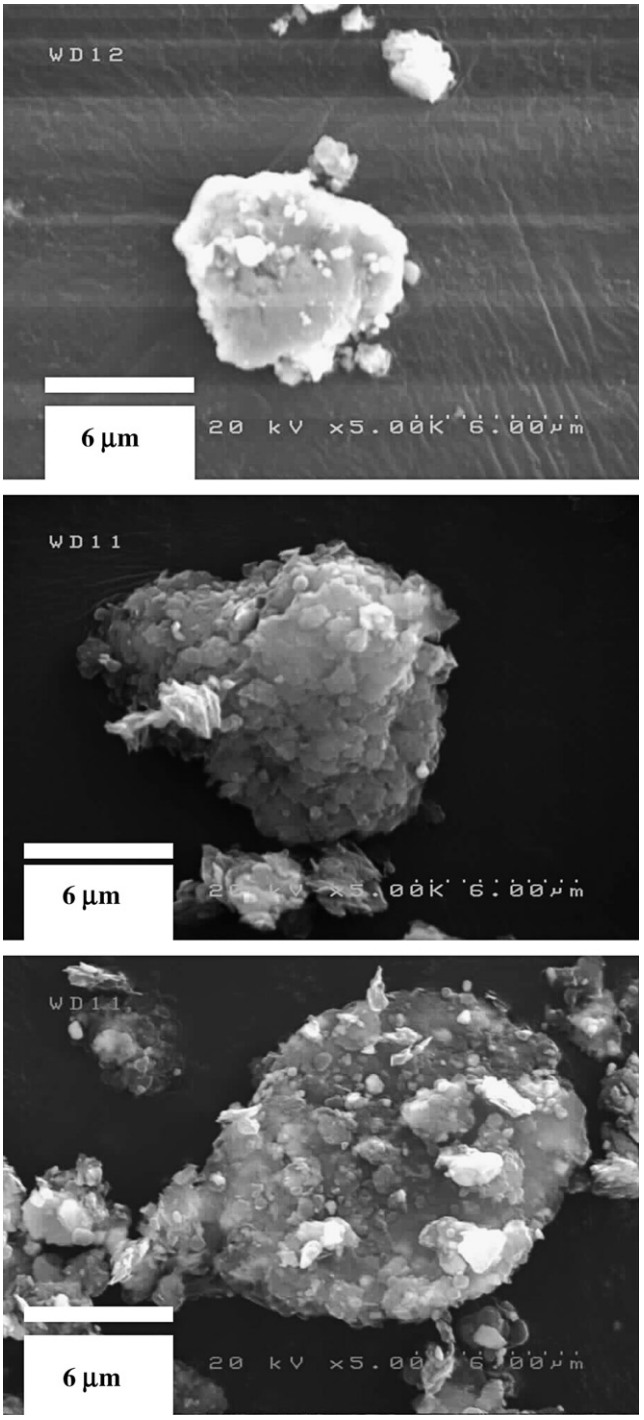

Fig. 4. Scanning electron microscopic images of (a) $FeSi_2$ alloy, (b) $FeSi_2$/graphite composite and (c) carbon coated $FeSi_2$ alloy.

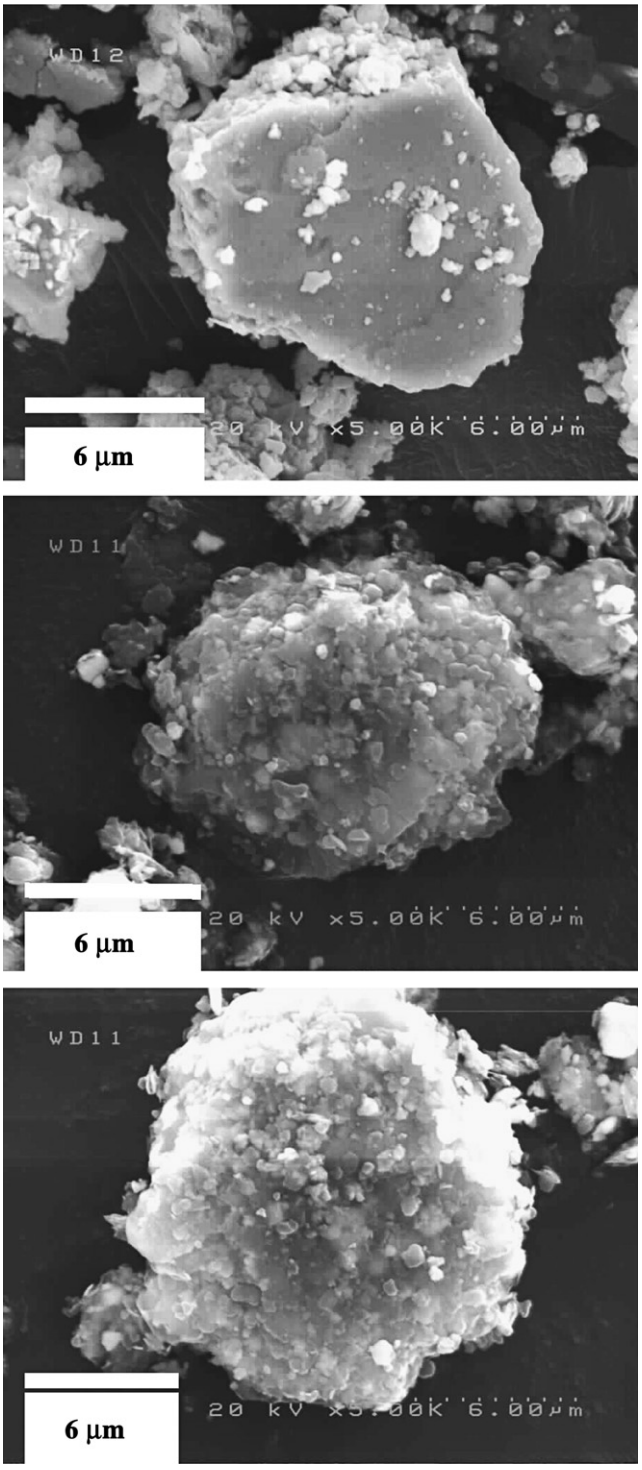

Fig. 5. Scanning electron microscopic images of (a) $Fe_{0.92}Mn_{0.08}Si_2$ alloy, (b) $Fe_{0.92}Mn_{0.08}Si_2$/graphite composite and (c) carbon coated $Fe_{0.92}Mn_{0.08}Si_2$ alloy.

their corresponding carbon, graphite composite particles against particle agglomeration, as understood further from SEM and particle size analysis studies.

3.3. Electrochemical property − charge−discharge study

Despite the demonstrated maximum capacity, silicon as an elemental anode in lithium-ion battery is reported to suffer from a high irreversible capacity and an unacceptable capacity fade due to ridiculous pulverization reaction. On the contrary, the present study that deals with the variety of silicon based alloy anodes and their suitable derivatives is expected to exhibit an improved electrochemical property with an acceptable capacity retention. In order to examine the same, the electrochemical performance of all the synthesized anode materials

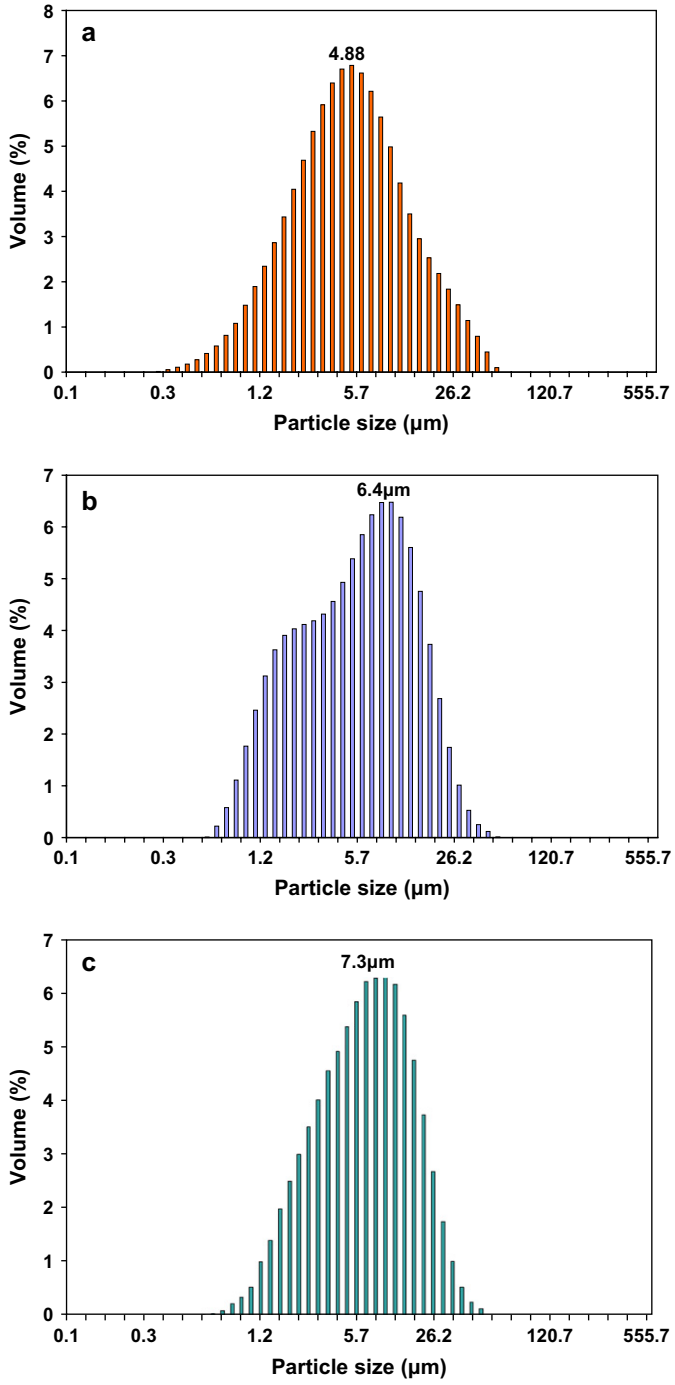

Fig. 6. Particle size distribution plot of (a) $FeSi_2$ alloy, (b) $FeSi_2$/graphite composite and (c) carbon coated $FeSi_2$ alloy.

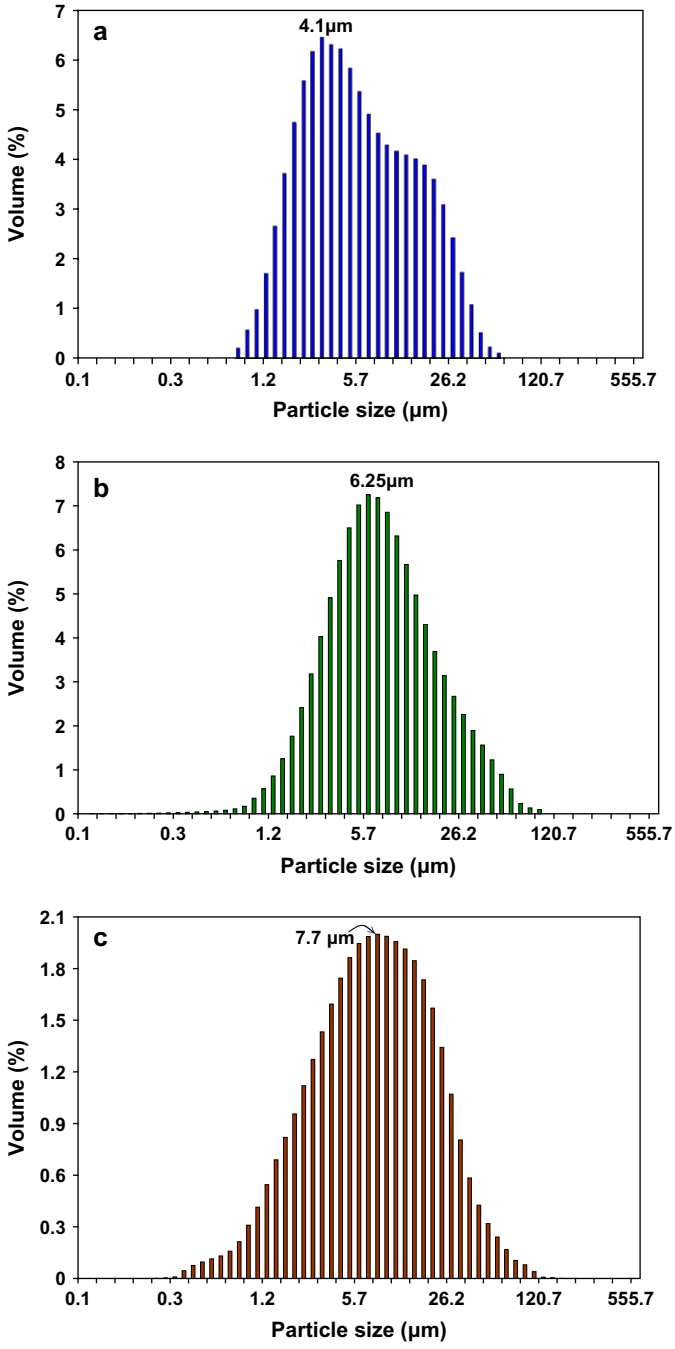

Fig. 7. Particle size distribution plot of (a) $Fe_{0.92}Mn_{0.08}Si_2$ alloy, (b) $Fe_{0.92}Mn_{0.08}Si_2$/graphite composite and (c) carbon coated $Fe_{0.92}Mn_{0.08}Si_2$ alloy.

was measured by deploying them individually as working electrodes against lithium metal counter electrode under a constant current drain of 0.5 mAh. The observed specific capacity values and the Ah efficiency values exhibited by different anodes at various cycles are tabulated (Table 1).

As far as the alloy anodes are concerned, $Fe_{0.92}Mn_{0.08}Si_2$ anode displayed an initial capacity of 1337 mAh/g (Fig. 9a) against $FeSi_2$ which showed only 972 mAh/g (Fig. 8a) with a very high irreversible capacity and severe capacity fade as experienced by Lee et al. [24]. The rapid loss in the reversible capacity of the native alloy may be attributed to the poor electron conductivity of silicon in its natural state [25]. However, manganese when incorporated as a dopant plays a vital role in enhancing the conductivity of the native alloy from 972 mAh/g to 1337 mAh/g (Figs. 8a and 9a), which is a significant improvement realized due to the effect of Mn doping. However, the effect of dopant (Mn) to improve or to modify the electrochemical properties of $FeSi_2$ anode is less beneficial compared to the effect of composite anode synthesized with $FeSi_2$ alloy. Because, despite the higher specific capacity values exhibited

Table 1
Comparison of electrochemical charge–discharge characteristics exhibited by $FeSi_2$ and $Fe_{0.92}Mn_{0.08}Si_2$ alloy anodes along with their suitably modified derivatives [observed specific capacity Q_c and Q_d in mAh/g and Ah efficiency values η in %]

Compound	Q_{c1}	Q_{d1}	η_1	Q_{c10}	Q_{d10}	η_{10}	Q_{c20}	Q_{d20}	η_{20}	Q_{c25}	Q_{d25}	η_{25}
$FeSi_2$	972	736	75	*	*	*	*	*	*	*	*	*
Carbon coated $FeSi_2$	148	128	86	148	144	97	169	166	98	177	174	98
$FeSi_2$/graphite	365	335	92	349	329	95	323	315	97	312	309	99
$Fe_{0.92}Mn_{0.08}Si_2$	1337	1020	76	*	*	*	*	*	*	*	*	*
C coated $Fe_{0.92}Mn_{0.08}Si_2$	209	192	91	193	190	97	191	185	96	190	184	97
$Fe_{0.92}Mn_{0.08}Si_2$/graphite	547	506	92	469	462	98	433	423	98	425	410	96

* – insignificant specific capacity values.

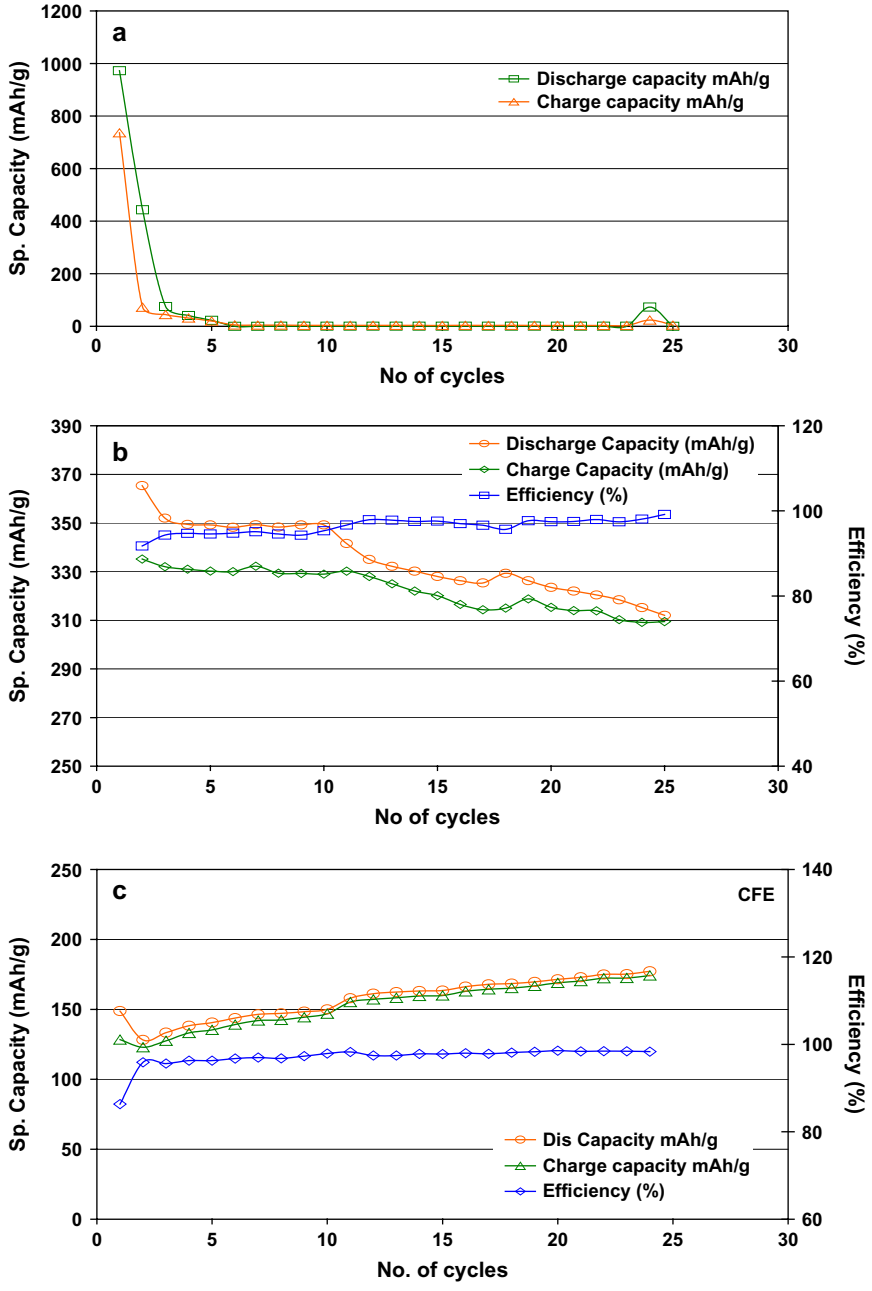

Fig. 8. Capacity vs cycleability behavior of (a) $FeSi_2$ alloy, (b) $FeSi_2$/graphite composite and (c) carbon coated $FeSi_2$ alloy.

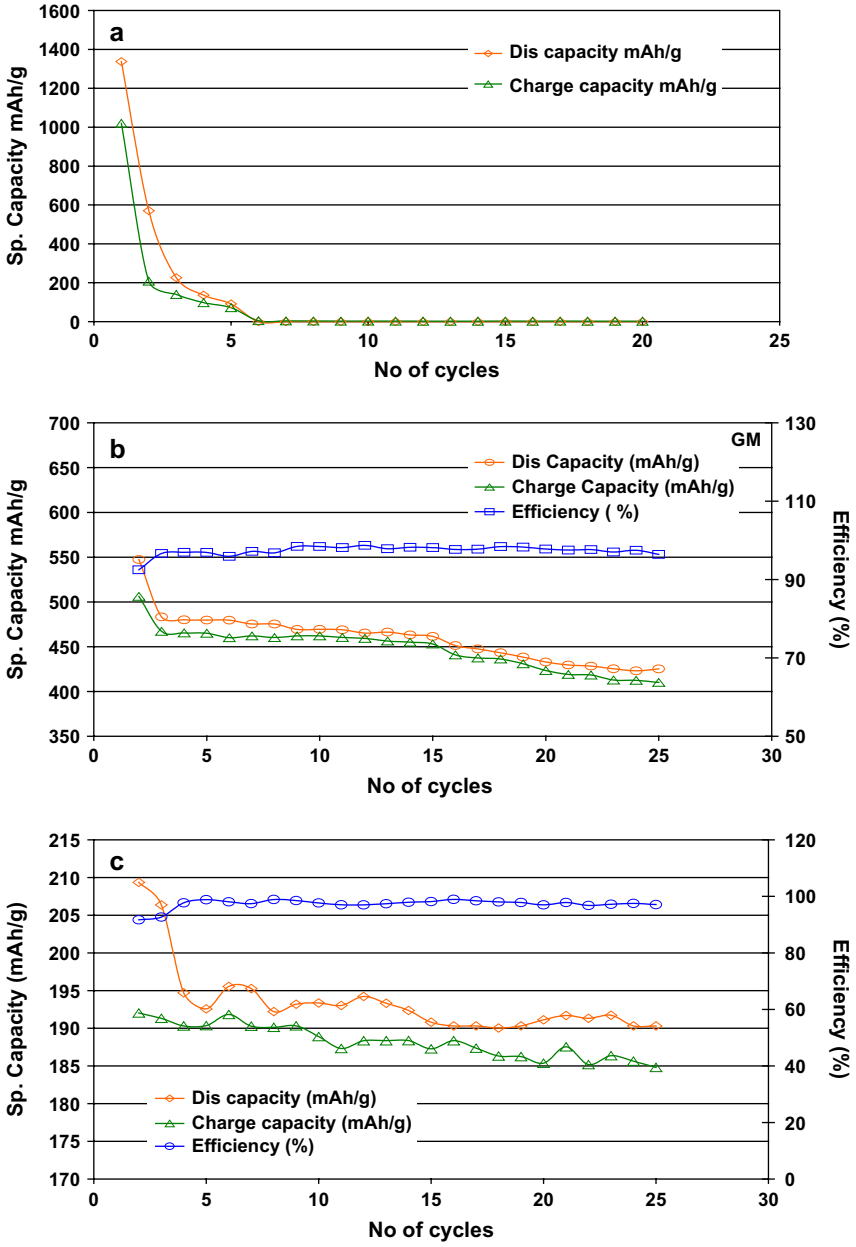

Fig. 9. Capacity vs cycleability behavior of (a) $Fe_{0.92}Mn_{0.08}Si_2$ alloy, (b) $Fe_{0.92}Mn_{0.08}Si_2$/graphite composite and (c) carbon coated $Fe_{0.92}Mn_{0.08}Si_2$ alloy.

by $Fe_{0.92}Mn_{0.08}Si_2$ anode (>1000 mAh/g), it was found to suffer seriously from severe capacity fade, as no significant capacity values were realized upon extended cycling (Table 1).

Alternatively, it is quite interesting to note that due to the buffering activity of the metal silicide and the added graphite, the specific capacity of $FeSi_2$/graphite and $Fe_{0.92}Mn_{0.08}Si_2$/graphite composite anodes was found to be 365 mAh/g and 547 mAh/g (Figs. 8b and 9b). Graphite, accompanied by the inactive matrix, has revealed an enhanced capacity with a reversible capacity of 340 mAh/g in case of $FeSi_2$ and 483 mAh/g from $Fe_{0.92}Mn_{0.08}Si_2$, along with an excellent coulombic efficiency of 95% and 98%, respectively. Also, the observed high coulombic efficiency (95–98%) values were found to get maintained upon progressive cycling (Table 1), which is attributed to the improved electrochemical effect of the composite anodes due to the added graphite. Thus, it is demonstrated that the effect of composite alloy anodes ($FeSi_2$/graphite and $Fe_{0.92}Mn_{0.08}Si_2$/graphite) is superior compared to that of the doped alloy anode ($Fe_{0.92}Mn_{0.08}Si_2$) in enhancing the overall electrochemical characteristics of native $FeSi_2$ anode.

Similarly, carbon coated alloy anodes exhibited excellent coulombic efficiency values constantly, even upon extended cycling, irrespective of the slightly reduced initial specific capacity values (Figs. 8c and 9c). This behavior is an indication that the treatment of carbon coating has improved the conductive contact between the active (Si) and inactive ($FeSi_2$ and Mn:Si) matrix in the alloy particles along with surface modification that enhances the capacity retention behavior of carbon coated alloy upon progressive cycling [19]. Interestingly, carbon coated $FeSi_2$ alloy and $Fe_{0.92}Mn_{0.08}Si_2$

anodes showed an initial capacity of 148 mAh/g and 210 mAh/g, respectively, with a significant capacity fade only after 15 cycles (Figs. 8c and 9c).

Similar to the reported efforts that deal with the possibility of improving the interface strength between electrode active material and current collector through post-heat treatment [25], the present study also substantiates the practically enhanced interface strength of alloy anodes, via carbon coating upon $FeSi_2$ and $Fe_{0.92}Mn_{0.08}Si_2$ matrix. Hence, the capacity retention capability has enhanced from 86% to 95% in the second cycle itself and thereafter to the extent of 98%, which is a remarkable improvement observed with the carbon coated $FeSi_2$ and $Fe_{0.92}Mn_{0.08}Si_2$ anodes (Figs. 8c and 9c). Such an improvement with respect to capacity retention and maintenance of structural stability upon cycling (Fig. 8c) could result from an enhanced interface strength between the entire part of the active material and the current collector. Because, stress on the interfaces between the layers of $FeSi_2$ and $Fe_{0.92}Mn_{0.08}Si_2$ alloys by the swelling of active materials is decreased due to the pyrolysed disordered carbon coating performed on the surface of respective alloys. As a result, separation of active material from the interface of each layer is suppressed, which is essential for the maintenance of specific capacity upon extended cycling. Thus, the process of carbon coating controls the fining of entire active material, its reaction with the electrolytes and the decrease of electronic conductivity among the active material and between themselves and the current collector so that the cycle performance is improved ultimately.

4. Conclusion

A set of $FeSi_2$, $FeSi_2$/graphite, carbon coated $FeSi_2$ and $Fe_{0.92}Mn_{0.08}Si_2$, $Fe_{0.92}Mn_{0.08}Si_2$/graphite, carbon coated $Fe_{0.92}Mn_{0.08}Si_2$ anodes were synthesized and investigated for electrochemical performance as anodes for Li-ion battery. $FeSi_2$ and $Fe_{0.92}Mn_{0.08}Si_2$ alloy anodes exhibited higher initial and reversible specific capacity (>1000 mAh/g) and insignificant progressive capacity values, implying that the effect of dopant has modified the electrochemical property of native $FeSi_2$ only partially. However, $FeSi_2$/graphite and $Fe_{0.92}Mn_{0.08}Si_2$/graphite composite anodes have exhibited excellent coulombic efficiency values, even upon extended cycling. Similarly carbon coated $FeSi_2$ and $Fe_{0.92}Mn_{0.08}Si_2$ anodes demonstrated better reversible capacity values, substantiating the role of carbon in enhancing the contact between active material and current collector. Hence it is concluded that the buffering action of graphite and the fining of electrode active material due to carbon coating are found to improve the overall electrochemical activity of native $FeSi_2$ and $Fe_{0.92}Mn_{0.08}Si_2$ anodes in a favorable manner, especially upon successive cycling.

References

[1] Winter M, Besenhard JO. Electrochim Acta 1991;45:31.
[2] Huggins RA. J Power Sources 1999;81–82:13.
[3] Besenhard JO, Yang J, Winter M. J Power Sources 1997;68:87–90.
[4] Manev V, Naidenov I, Puresheva B, Pistoia G. J Power Sources 1995;57:133.
[5] Kuwabata S, Tsumura N, Goda S, Martin CR, Yoneyama H. J Electrochem Soc 1998;145:1415.
[6] Wen CJ, Huggins RA. J Solid State Chem 1976;37:271.
[7] Seefurth RN, Sharma RA. J Electrochem Soc 1977;124:1207.
[8] Lee Ki-Lyoung, Jung Ju-Young, Lee Seung-Won, Moon Hee-Soo, Park Jong-Wan. J Power Sources 2004;129:270–4.
[9] Takamura Tsutomu, Ohara Shigeki, Uehara Makiko, Suzuki Junji, Sekine Kyoichi. J Power Sources 2004;129:96–100.
[10] Zaghib Karim, Kinoshita Kimio. J Power Sources 2004;125:214–20.
[11] Wolfenstine J. J Power Sources 2003;124:241–5.
[12] Yoshio Masaki, Tsumura Takaaki, Dimov Nikolay. J Power Sources 2005;146:10–4.
[13] Dimov N, Kugino S, Yoshio M. J Power Sources 2004;136:108–14.
[14] Dimov Nikolay, Kugino Satoshi, Yoshio Masaki. Electrochim Acta 2003;48:1579–87.
[15] Zhang Xiang-Wu, Patil Prashanth K, Wang Chunsheng, Appleby AJohn, Little Frank E, Cocke David L. J Power Sources 2004;125:206–13.
[16] Umeno T, Fukuda K, Wang H, Dimov N, Yoshio M. Chem Lett 2001;1186.
[17] Lee S, Lee J, Chung S, Lee H, Lee S, Baik H. J Power Sources 2001; 97–98:191.
[18] Li H, Huang XJ, Chen LQ, Wu ZG, Liang Y. Electrochem Solid-State Lett 1999;2:547.
[19] Dong H, Ai XP, Yang HX. Electrochem Commun 2003;5:952–7.
[20] Jayaprakash N, Doh CH, Kalaiselvi N. Communicated and unpublished results.
[21] Lee HY, Back JK, Jang SW, Lee SM, Hong ST, Lee KY, et al. J Power Sources 2001;101:206.
[22] Patel P, Kim IS, Maranchi J, Kumta P. J Power Sources 2004;135:273.
[23] Ur Soon-Chul, Kim Il Ho. Met Mater 2005;11:301–8.
[24] Lee Heon-Yong, Kim Young-Lae, Hong Moon-Ki, Lee Sung-Man. J Power Sources 2005;141:159–62.
[25] Hanai K, Liu Y, Imanishi N, Hirano A, Matsumura M, Ichikawa T, et al. J Power Sources 2005;146:156–60.